

## Phthalazine-Based Dinucleating Ligands Afford Dinuclear Centers Often Encountered in Metalloenzyme Active Sites

Amy M. Barrios and Stephen J. Lippard\*

Department of Chemistry, Massachusetts Institute of Technology, Cambridge, Massachusetts 02139

Received August 4, 2000

### Introduction

Enzymes having two metal ions at their active sites catalyze diverse reactions ranging from alkane oxidation to biopolymer degradation.<sup>1–4</sup> These metalloenzymes utilize many of the first-row transition metal ions to effect the desired transformation at both homo- and heterodimetallic centers. For example, hydroxide-bridged dizinc(II) centers hydrolyze phosphate esters<sup>5</sup> and peptide bonds,<sup>2</sup> and steps in nitrogen metabolism are catalyzed by the dimanganese(II) enzyme arginase<sup>6</sup> and the dinickel(II) center in urease.<sup>7</sup> Crucial oxidation reactions are also performed in vivo by dinuclear metalloenzymes. Examples include alkane oxidation at diiron centers in methane monooxygenase<sup>8</sup> and alkane desaturases<sup>3</sup> and the disproportionation of hydrogen peroxide by the dimanganese enzyme, catalase.<sup>4</sup> Considerable research has been directed toward developing a better understanding of these metalloenzymes.<sup>3,8,9</sup> Such information would not only provide insight into the fundamental chemistry achieved by these enzymes but also might facilitate the design of potential inhibitors that could be useful for treating the pathological effects mediated by some of them. Ultimately, chemists might be able to design new biomimetic catalysts for use in synthetic, industrial, and other applications.<sup>10–12</sup>

One way to gain insight into reactions catalyzed by dinuclear metalloenzymes is through the design of synthetic model complexes that mimic the structural and/or functional properties of the enzyme of interest. The choice of ligand is driven in part by the goals of the modeling study.<sup>13</sup> If a close structural model of the enzyme active site is desired, ligands similar to the biological donors at the enzyme active site, such as carboxylates and imidazoles, should be used. Functional enzyme models may not need to reproduce exactly the structural features of the active site. Instead, a dinucleating ligand that holds two metal ions in proximity with relatively high kinetic stability while leaving coordination sites available for substrate and/or nucleophile

binding can often be desirable. Many different ligands have been designed for such a purpose.<sup>13–16</sup>

One such set of ligands is based on the phthalazine framework. Dinucleating ligands in this class promote the formation of dinuclear nickel and copper complexes.<sup>14,17,18</sup> The reactivity of these complexes had not been extensively explored, however, and phthalazine-bridged complexes of other transition metals were not investigated prior to our work in this area. As described previously, we have employed the ligand 1,4-bis(2,2'-dipyridylmethyl)phthalazine (bdptz)<sup>19</sup> to model the dinickel(II) center in urease. The phthalazine moiety, although electronically distinct from carboxylate ligands often encountered in enzymes, serves a similar purpose in bringing two metal ions into proximity. The pyridine donor arms of bdptz mimic histidine residues at the active sites of many such metalloenzymes.

In this short note we present the results of exploratory work that demonstrates a broader utility of phthalazine-based ligand systems as frameworks for the syntheses of dinuclear metal complexes that model the structural and functional aspects of metalloenzymes. Dinuclear manganese, iron, copper, and zinc complexes of the bdptz ligand were obtained that display a range of metal–metal distances and the ability to bind a variety of exogenous ligands. We suggest that the combination of structural stability and flexibility afforded by the dinuclear bdptz platform makes this and related ligands well suited for use in modeling the reactivity of metalloenzyme active sites.

### Experimental Section

**General Considerations.** 1,4-Bis(2,2'-dipyridylmethyl)phthalazine (bdptz)<sup>19</sup> and 2,6-di(*p*-tolyl)benzoic acid (HO<sub>2</sub>CAr')<sup>20–22</sup> were synthesized according to literature procedures. The manipulation of air-sensitive compounds was performed in a nitrogen-filled Vacuum Atmospheres glovebox. Diethyl ether and acetonitrile for use in the glovebox were distilled under nitrogen from benzophenone ketyl and CaH<sub>2</sub>, respectively.

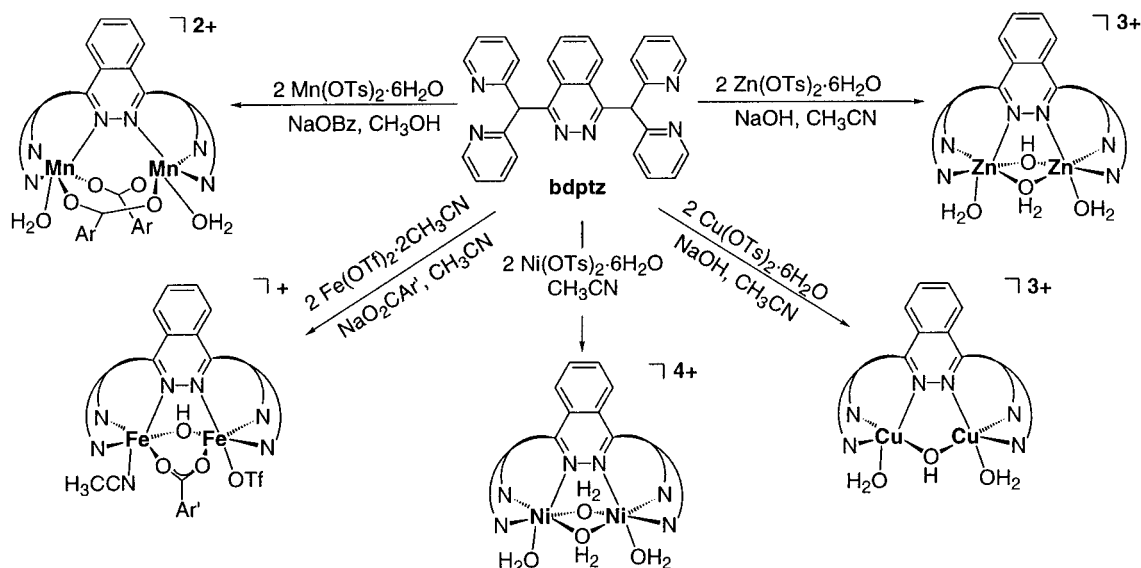
**Physical Methods.** FTIR spectra of the complexes were obtained from samples pressed into KBr pellets measured by an FTS-135 FTIR spectrometer. A Hewlett-Packard 8453-A diode array spectrophotometer was used to obtain electronic spectra. NMR data were collected on a Unity 300 MHz NMR spectrometer.

**[Mn<sub>2</sub>(μ-OBz)<sub>2</sub>(bdptz)(H<sub>2</sub>O)<sub>2</sub>](OTs)<sub>2</sub> (1).** A 124 mg, 248 μmol aliquot of [Mn(H<sub>2</sub>O)<sub>6</sub>](OTs)<sub>2</sub> was dissolved in 2 mL of 10:1 acetonitrile/water. A 53 mg, 113 μmol portion of bdptz and a 27 mg, 187 μmol portion of sodium benzoate were alternately added to the aqueous acetonitrile solution in small portions (each ligand was divided into approximately 3 equal parts). After the solution was stirred for a few minutes, a yellow solid precipitated. The solid was collected by filtration and washed with acetone. The isolated yield of **1** was 78 mg (58%), and the yellow powder was recrystallized from diethyl ether vapor diffusion into a methanolic solution of **1** to produce X-ray quality

- (1) Wilcox, D. E. *Chem. Rev.* **1996**, *96*, 2435–2458.
- (2) Taylor, A. *TIBS* **1993**, *18*, 167–172.
- (3) Kurtz, D. M. *JBIC, J. Biol. Inorg. Chem.* **1997**, *2*, 159–167.
- (4) Dismukes, G. C. *Chem. Rev.* **1996**, *96*, 2909–2926.
- (5) Vanhooke, J. L.; Benning, M. M.; Raushel, F. M.; Holden, H. M. *Biochem.* **1996**, *35*, 6020–6025.
- (6) Kanyo, Z. F.; Scolnick, L. R.; Ash, D. E.; Christianson, D. W. *Nature* **1996**, *383*, 554–557.
- (7) Jabri, E.; Carr, M. B.; Hausinger, R. P.; Karplus, P. A. *Science* **1995**, *268*, 998–1004.
- (8) Valentine, A. M.; Lippard, S. J. *J. Chem. Soc., Dalton Trans.* **1997**, 3925–3931.
- (9) Wieghardt, K. *Angew. Chem., Int. Ed. Engl.* **1989**, *28*, 1153–1172.
- (10) Suh, J. *Acc. Chem. Res.* **1992**, *25*, 273–279.
- (11) Breslow, R. *Acc. Chem. Res.* **1995**, *28*, 146–153.
- (12) Göbel, M. W. *Angew. Chem., Int. Ed. Engl.* **1994**, *33*, 1141–1143.
- (13) Fenton, D. E. *Chem. Soc. Rev.* **1999**, *28*, 159–168.

- (14) Robichaud, P.; Thompson, L. K. *Inorg. Chim. Acta* **1984**, *85*, 137–142.
- (15) Thompson, L. K.; Mandal, S. K.; Rosenberg, L.; Lee, F. L.; Gabe, E. *J. Inorg. Chim. Acta* **1987**, *133*, 81–91.
- (16) Watton, S. P.; Masschelein, A.; Rebek, J., Jr.; Lippard, S. J. *J. Am. Chem. Soc.* **1994**, *116*, 5196–5205.
- (17) Sullivan, D. A.; Palenik, G. J. *Inorg. Chem.* **1977**, *16*, 1127–1133.
- (18) Thompson, L. K.; Chako, V. T.; Elvidge, J. A.; Lever, A. B. P.; Parish, R. V. *Can. J. Chem.* **1969**, *47*, 4141–4152.
- (19) Barrios, A. M.; Lippard, S. J. *J. Am. Chem. Soc.* **1999**, *121*, 11751–11757.
- (20) Du, C.-J. F.; Hart, H.; Ng, K.-K. D. *J. Org. Chem.* **1986**, *51*, 3162–3165.
- (21) Chen, C.-T.; Siegel, J. S. *J. Am. Chem. Soc.* **1994**, *116*, 5959–5960.
- (22) Saednya, A.; Hart, H. *Synthesis* **1996**, 1455–1458.

Scheme 1



crystals. FTIR (KBr,  $\text{cm}^{-1}$ ): 3326 (br), 3061 (w), 3028 (w), 2938 (w), 2971 (w), 2820 (w), 1668 (m), 1603 (s), 1560 (s), 1491 (m), 1472 (m), 1443 (s), 1410 (s), 1205 (s), 1167 (s), 1113 (m), 1034 (s), 1007 (s), 810 (m), 775 (m), 721 (m), 679 (m), 640 (w), 559 (m). UV-vis ( $\text{CH}_3\text{CN}$ ) ( $\lambda$ , nm ( $\epsilon$ ,  $\text{M}^{-1} \text{cm}^{-1}$ )): 223 (80 000), 258 (sh, 16 800), 263 (18 600), 270 (sh, 16 200). Anal. Calcd for  $\text{Mn}_2\text{C}_{60}\text{H}_{58}\text{N}_6\text{O}_{14}\text{S}_2$  (**1**·2MeOH): C, 57.14; H, 4.64; N, 6.66. Found: C, 57.11; H, 4.36; N, 6.86.

**[Fe<sub>2</sub>( $\mu$ -OH)( $\mu$ -O<sub>2</sub>CAr')(bdptz)(OTf)(CH<sub>3</sub>CN)](OTf) (2)**. A 145 mg, 330  $\mu\text{mol}$  portion of  $\text{Fe}(\text{OTf})_2 \cdot 2\text{CH}_3\text{CN}$  was dissolved in acetonitrile under an inert atmosphere. Equimolar amounts of solid bdptz (75 mg, 160  $\mu\text{mol}$ ) and  $\text{NaO}_2\text{CAr}'$  (52 mg, 160  $\mu\text{mol}$ ), where  $\text{O}_2\text{CAr}'$  is 2,6-di(*p*-tolyl)benzoate, were mixed thoroughly and added to the iron triflate solution as a mixture of solids in several small portions with stirring. After the reaction mixture was stirred for 1 h, 1 equiv of lithium hydroxide was added as a solid and the mixture was stirred for an additional hour to allow all of the solid to dissolve. To the resulting deep red-purple acetonitrile solution was added a few drops of dichloromethane and the mixture was exposed to diethyl ether by vapor diffusion, which produced deep red-brown crystals of **2** in 70% yield. FTIR (KBr,  $\text{cm}^{-1}$ ): 3070 (w), 3031 (w), 2969 (w), 2932 (w), 2868 (w), 2278 (w), 1597 (s), 1567 (s), 1443 (m), 1383 (w), 1257 (br, s), 1157 (m), 1031 (s), 766 (s), 637 (s), 571 (m). UV-vis ( $\text{CH}_3\text{CN}$ ) ( $\lambda$ , nm ( $\epsilon$ ,  $\text{M}^{-1} \text{cm}^{-1}$ )): 380 (2700), 420 (2600), 515 (2900). Anal. Calcd for  $\text{Fe}_2\text{C}_{61}\text{H}_{57}\text{N}_7\text{O}_{16}\text{S}_2\text{F}_6\text{Cl}_4$  ( $2 \cdot \text{Et}_2\text{O} \cdot 2\text{CH}_2\text{Cl}_2$ ): C, 49.51; H, 3.88; N, 6.63. Found: C, 49.21; H, 3.84; N, 6.43.

**[Fe<sub>2</sub>( $\mu$ -O)( $\mu$ -O<sub>2</sub>CAr')(bdptz)(acetone)(OTf)](OTf)<sub>2</sub> (3)**. A 6.67  $\mu\text{mol}$  solution of **2** in acetonitrile was cooled to  $-40^\circ\text{C}$  in a quartz Dewar. The electronic spectrum of **2** was measured before and after dioxygen was bubbled through the solution. Upon exposure to dioxygen, the diiron(II) complex **2** was converted into the diiron(III) complex **3** without any observable intermediates. Recrystallization of **3** from diethyl ether by vapor diffusion into a 20:1 acetone/chlorobenzene solution produced X-ray quality crystals. FTIR (KBr,  $\text{cm}^{-1}$ ): 3088 (w), 3055 (w), 3019 (w), 2926 (w), 1606 (s), 1560 (m), 1447 (m), 1290 (s), 1215 (br, s), 1158 (s), 1028 (vs), 758 (m), 636 (s). UV-vis ( $\text{CH}_3\text{CN}$ ) ( $\lambda$ , nm ( $\epsilon$ ,  $\text{M}^{-1} \text{cm}^{-1}$ )): 345 (7000, sh), 380 (5600, sh), 518 (1106). Anal. Calcd for  $\text{Fe}_2\text{C}_{66}\text{H}_{56}\text{N}_6\text{O}_{14}\text{S}_3\text{F}_6\text{Cl}$  (**3**·chlorobenzene·acetone): C, 50.44; H, 3.59; N, 5.35. Found: C, 50.81; H, 3.53; N, 5.85.

**[Cu<sub>2</sub>( $\mu$ -OH)(bdptz)(H<sub>2</sub>O)<sub>2</sub>](OTf)<sub>3</sub> (4)**. To an aqueous acetonitrile (1:10) solution of 109 mg, 212  $\mu\text{mol}$  of copper tosylate was added a 50 mg, 106  $\mu\text{mol}$  portion of bdptz with stirring. After the turquoise-blue solution was stirred for a few minutes, 1 equiv of a 1.0 M NaOH solution was added in a dropwise manner. The resulting solution was exposed to diethyl ether by vapor diffusion, producing X-ray quality turquoise crystals in 42% yield. FTIR (KBr,  $\text{cm}^{-1}$ ): 3407 (br), 3094 (w), 3055 (w), 1651 (m), 1609 (s), 1595 (s), 1491 (w), 1474 (m), 1443

(s), 1362 (w), 1198 (br, s), 1123 (m), 1035 (s), 1010 (s), 820 (m), 775 (m), 681 (s), 566 (m). UV-vis ( $\text{CH}_3\text{CN}$ ) ( $\lambda$ , nm ( $\epsilon$ ,  $\text{M}^{-1} \text{cm}^{-1}$ )): 650 (70), 960 (31). Anal. Calcd for  $\text{Cu}_2\text{C}_{51}\text{H}_{56}\text{N}_6\text{O}_{16}\text{S}_3$  (**4**·4H<sub>2</sub>O): C, 49.71; H, 4.58; N, 6.82. Found: C, 49.99; H, 4.42; N, 6.85.

**[Zn<sub>2</sub>( $\mu$ -OH)( $\mu$ -H<sub>2</sub>O)(bdptz)(H<sub>2</sub>O)<sub>2</sub>](OTf)<sub>3</sub> (5)**. A 119 mg, 231  $\mu\text{mol}$  portion of zinc tosylate was dissolved in 10:1 acetonitrile/water with stirring and gentle heating. To this solution was added 52 mg, 111  $\mu\text{mol}$  of bdptz followed by 1 equiv of a 1.0 M NaOH solution. Colorless crystals of **5** were obtained by exposing the resulting solution to diethyl ether by vapor diffusion. The crystalline product was obtained in 51% yield. FTIR (KBr,  $\text{cm}^{-1}$ ): 3424 (br), 3073 (w), 2923 (w), 1648 (m), 1604 (s), 1570 (m), 1560 (m), 1508 (w), 1476 (w), 1444 (m), 1365 (w), 1200 (br, s), 1122 (m), 1036 (s), 1011 (s), 817 (w), 778 (w), 684 (m), 568 (w). UV-vis ( $\text{CH}_3\text{CN}$ ) ( $\lambda$ , nm ( $\epsilon$ ,  $\text{M}^{-1} \text{cm}^{-1}$ )): 225 (61 500), 264 (20 000), 271 (sh, 17 500), 295 (sh, 2800). <sup>1</sup>H NMR ( $\text{CD}_3\text{CN}$ ):  $\delta$  9.15 (m, 4H), 8.95 (d,  $J = 6$  Hz, 4H), 8.34 (m, 4H), 8.03 (d,  $J = 9$  Hz, 4H), 7.92 (t,  $J = 8$  Hz, 4H), 7.62 (d,  $J = 9$  Hz, 6H), 7.46 (t,  $J = 7$  Hz, 4H), 7.10 (d,  $J = 9$ , 6H), 7.04 (s, 2H), 2.32 (s, 9H). Anal. Calcd for  $\text{Zn}_2\text{C}_{51}\text{H}_{62}\text{N}_6\text{O}_{19}\text{S}_3$  (**5**·6H<sub>2</sub>O): C, 47.48; H, 4.84; N, 6.51. Found: C, 47.72; H, 4.82; N, 6.55.

**Collection and Reduction of X-ray Data.** Procedures for the collection and reduction of X-ray data have been reported previously.<sup>23</sup> In brief, the crystals were mounted on the tips of glass fibers with Paratone-N (Exxon) and cooled rapidly in the  $-85^\circ\text{C}$  cold stream of a Bruker (formerly Siemens) CCD X-ray diffractometer controlled by a Pentium based PC running the SMART<sup>24</sup> software package. The structures were solved by using the direct-methods programs XS or SIR, part of the SHELXTL<sup>25</sup> or TEXSAN<sup>26</sup> program packages, respectively, and refinements were carried out using XL. All non-hydrogen atoms were refined by a series of least-squares cycles. Hydrogen atoms were assigned to idealized positions and given a thermal parameter 1.2 times that of the atom to which they are attached, except for **5** where all were located and refined isotropically. Empirical absorption corrections were calculated and applied for each structure using the program SADABS,<sup>27</sup> and PLATON<sup>28</sup> was used to search for

(23) Feig, A. L.; Bautista, M. T.; Lippard, S. J. *Inorg. Chem.* **1996**, *35*, 6892–6898.

(24) SMART, versuib 5.05; Bruker AXS, Inc.: Madison, WI, 1998.

(25) Sheldrick, G. M. *SHELXTL: Program for the Refinement of Crystal Structures*, 97-2 ed.; University of Göttingen: Göttingen, Germany, 1997.

(26) TEXSAN: *Single-Crystal Structure Analysis Software*; Molecular Structure Corporation: The Woodlands, TX, 1995.

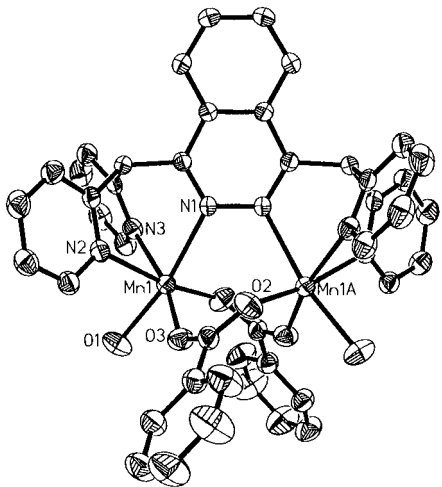
(27) Sheldrick, G. M. *SADABS: Area-Detector Absorption Correction*; University of Göttingen: Göttingen, Germany, 1996.

(28) Spek, A. L. *PLATON, A Multipurpose Crystallographic Tool*; Utrecht University: Utrecht, The Netherlands, 1998.

**Table 1.** Summary of X-ray Crystallographic Data

	1·2CH <sub>3</sub> OH	3·2CH <sub>3</sub> CN·MeOH	4·CH <sub>3</sub> CN·4H <sub>2</sub> O	5·8H <sub>2</sub> O
formula	C <sub>60</sub> H <sub>58</sub> N <sub>6</sub> O <sub>14</sub> Mn <sub>2</sub> S <sub>2</sub>	C <sub>62</sub> H <sub>57</sub> N <sub>8</sub> O <sub>24</sub> F <sub>9</sub> Fe <sub>2</sub> S <sub>3</sub>	C <sub>53</sub> H <sub>59</sub> N <sub>7</sub> O <sub>16</sub> Cu <sub>2</sub> S <sub>3</sub>	C <sub>51</sub> H <sub>66</sub> N <sub>6</sub> O <sub>21</sub> Zn <sub>2</sub> S <sub>3</sub>
fw	1261.12	1517.04	1273.33	1326.02
space group	C2/c	P $\bar{1}$	Pnma	P $\bar{1}$
a, Å	25.5882(15)	11.8858(1)	13.811(8)	13.111(4)
b, Å	11.2031(5)	14.9402(3)	25.107(14)	14.100(5)
c, Å	23.7301(10)	20.4129(1)	16.085(12)	17.757(6)
$\alpha$ , deg		88.076(1)		85.484(9)
$\beta$ , deg	118.122(1)	78.272(1)		69.552(12)
$\gamma$ , deg		69.418(1)		75.202(9)
V, Å <sup>3</sup>	5999.6(5)	3319.79(7)	5577(6)	2973.6(17)
Z	4	2	4	2
$\rho_{\text{calcd}}$ , g/cm <sup>3</sup>	1.396	1.518	1.516	1.481
temp, °C	-85	-85	-85	-85
$\mu$ (Mo K $\alpha$ ), mm <sup>-1</sup>	0.711	0.627	0.711	0.992
2 $\theta$ limits, deg	3-57	3-57	3-57	3-57
total no. data	18 525	20 923	33 795	26 631
no. unique data	6996	14 559	6752	13 305
obsd data <sup>a</sup>	5009	7785	5417	8909
no. parameters	373	937	496	1040
R <sup>b</sup>	0.0519	0.0782	0.0388	0.0423
wR2 <sup>c</sup>	0.1517	0.1795	0.1162	0.0808
max, min peaks, e/Å <sup>3</sup>	0.887, -0.709	0.647, -0.502	0.55, -0.971	0.484, -0.368

<sup>a</sup> Observation criterion:  $I > 2\sigma(I)$ . <sup>b</sup>  $R = \sum||F_o| - |F_c||/\sum|F_o|$ . <sup>c</sup>  $wR2 = \{\sum[w(F_o^2 - F_c^2)^2]/\sum[w(F_o^2)^2]\}^{1/2}$ .

**Table 2.** Selected Interatomic Distances (Å) and Angles (deg)


	1	3	4	5
M(1)···M(2)	3.754(2)	3.121(3)	3.190(2)	3.169(2)
M(1)-L(1)	2.169(2)	2.000(3)	1.973(2)	2.043(2)
M(1)-L(2)	2.127(2)	1.806(3)	1.894(2)	2.056(2)
M(1)-L(3)	2.100(2)	2.033(3)		2.405(2)
M(2)-L(4)		2.009(4)		2.035(2)
M(2)-L(2)		1.816(3)		2.051(2)
M(2)-L(3)		2.022(3)		2.296(2)
N(1)-M(1)-L(1)	167.84(9)	164.87(14)	178.31(8)	167.76(10)
N(2)-M(2)-L(4)		168.23(15)		179.17(10)
M(1)-L(2)-M(2)	N/A	119.05(17)	114.70(12)	100.96(10)
M(1)-L(3)-M(2)	N/A	N/A	N/A	84.73(8)

higher symmetry. Selected crystallographic information for compounds 1–5 can be found in Tables 1 and 2, and all pertinent crystallographic data are included in Tables S1–S25 in the Supporting Information.

## Results and Discussion

As demonstrated in Scheme 1 and Table 2, bdpztz is an effective dinucleating ligand that can be used with a variety of different metal ions. In all of these complexes, the ligand coordinates to the dimetallic center with the phthalazine moiety bridging the two metal ions and the pyridine arms of the ligand providing two terminal nitrogen donors to each metal. Two bridging positions and one terminal coordination site at each metal ion remain available for exogenous ligand binding. Intermetallic distances ranging from 3.121(3) to 3.754(3) Å are accommodated by this ligand system. In most of the complexes, two exogenous bridging ligands form additional links between the two metal ions. The M–M distance correlates with the nature of the bridging ligands. Complexes having two single atom bridges, such as hydroxide or water, generally exhibit shorter metal–metal separations than complexes with one or more multiple atom bridges, such as a  $\mu$ -1,3-carboxylate. As expected,

**Figure 1.** ORTEP diagram of the cation of 1, showing 50% probability ellipsoids. All hydrogen atoms have been omitted for clarity.

the ( $\mu$ -oxo)( $\mu$ -carboxylato)diiron(III) complex 3 provides an exception to this trend. Ligands in terminal coordination sites are usually solvent-derived and can easily be replaced by substrate molecules, as demonstrated for the dinickel bdpztz complexes described previously.<sup>19,29,30</sup>

The reaction of bdpztz with manganese(II) tosylate in the presence of 2 equiv of sodium benzoate produced [Mn<sub>2</sub>( $\mu$ -OBz)<sub>2</sub>(bdpztz)(H<sub>2</sub>O)<sub>2</sub>](OTs)<sub>2</sub> (1), the structure of which is shown in Figure 1. Each manganese ion has a pseudo-octahedral ligand environment with the phthalazine moiety and two benzoate ligands bridging the two metal ions. Two pyridine donor arms from the ligand coordinate to each metal, and the remaining terminal coordination sites are occupied by water molecules. The dimanganese(II) complex 1 is relatively stable to oxidation in part because of the nitrogen-rich environment afforded by the bdpztz ligand. In solution, 1 is stable for several days before forming an intractable brown product, and crystals of 1 are stable indefinitely in air.

(29) Barrios, A. M.; Lippard, S. J. *J. Am. Chem. Soc.* **2000**, *122*, 9172–9177.

(30) Barrios, A. M.; Lippard, S. J. *Inorg. Chem.*, in press.

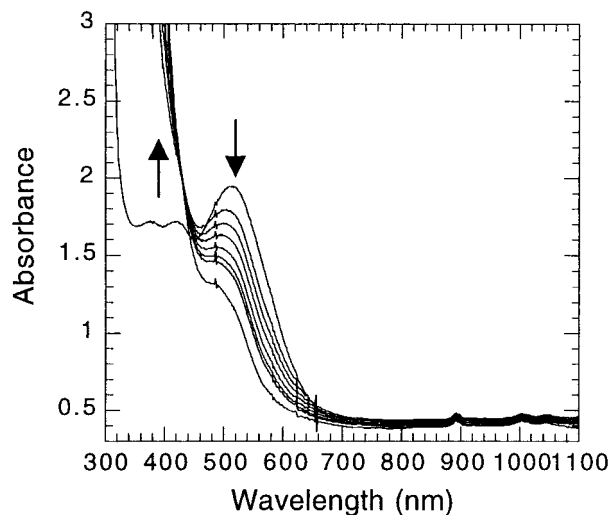


**Figure 2.** Electronic spectrum showing the conversion of an acetonitrile solution of **2** to **3** upon bubbling with dioxygen for 2 min at room temperature. The initial trace shows the reduced species, and subsequent traces were obtained between 2 min and 2 h after dioxygen exposure.

The singly carboxylate-bridged diiron(II) complex  $[\text{Fe}_2(\mu\text{-OH})(\mu\text{-O}_2\text{CAr}')(\text{bdptz})(\text{OTf})(\text{CH}_3\text{CN})](\text{OTf})$  (**2**) was synthesized by using a carboxylate ligand with sufficient steric bulk to prevent the formation of dicarboxylate-bridged species. In this complex (Scheme 1, Table 5), a hydroxide ion and the bulky carboxylate ligand bridge the two metal ions in addition to the phthalazine moiety. The terminal positions are asymmetrically occupied, with a triflate anion binding to one site and an acetonitrile molecule occupying the other. This asymmetry is introduced because the 2,6-di(*p*-tolyl)phenyl moiety of the carboxylate ligand is twisted relative to the plane of the carboxylate group. The aromatic ring and the carboxylate group are canted with respect to one another at a  $75^\circ$  angle. Consequently, the toluene moiety that points toward the terminal coordination sites of the metal ions is directed toward Fe(2) and slightly away from Fe(1). This positioning allows more space for the ligand terminally coordinated to Fe(1), resulting in binding of a triflate ion, whereas a sterically less demanding acetonitrile molecule binds to the terminal site of Fe(2).

Exposure of **2** to dioxygen results in conversion to  $[\text{Fe}_2(\mu\text{-O})(\mu\text{-O}_2\text{CAr}')(\text{bdptz})(\text{OTf})(\text{acetone})](\text{OTf})_2$  (**3**) with no detectable intermediates, even at  $-78^\circ\text{C}$ . The conversion of **2** to **3** upon exposure of a solution of **2** to dioxygen is reflected in the electronic spectra in Figure 2. Compound **3** is a diiron(III) complex bridged by the phthalazine moiety of bdptz, a carboxylate group, and an oxide ligand. An ORTEP diagram of **3** is shown in Figure 3. A triflate ion and a molecule of acetone occupy the terminal sites. The asymmetry in the terminal coordination sites is again due to a canting of the carboxylate ligand. In this complex, the dihedral angle between the carboxylate moiety and aromatic ring is  $68^\circ$ .

The dicopper(II) bdptz complex  $[\text{Cu}_2(\mu\text{-OH})(\text{bdptz})(\text{H}_2\text{O})_2](\text{OTs})_3$  (**4**) is the only bdptz complex in which the metal ions are not in a pseudo-octahedral coordination environment. Instead, each copper ion has square-pyramidal coordination geometry. An ORTEP diagram of **4** is presented in Figure 4. The two metal ions are bridged by the phthalazine moiety of the ligand, and a hydroxide ion and water molecule coordinate to each copper ion. The phthalazine moiety, the hydroxide ion, a water molecule, and one of the pyridine nitrogen atoms form the base of the square pyramid for each copper ion, with N(2) from the ligand occupying the apical position. An oxygen atom

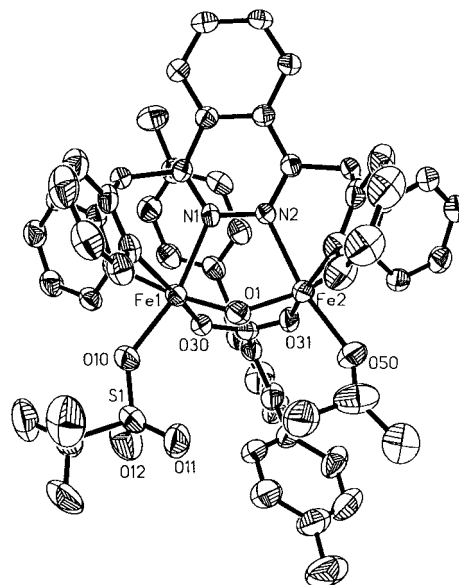


**Figure 3.** ORTEP diagram of the cation of **3**, showing 50% probability ellipsoids. All hydrogen atoms have been omitted for clarity.

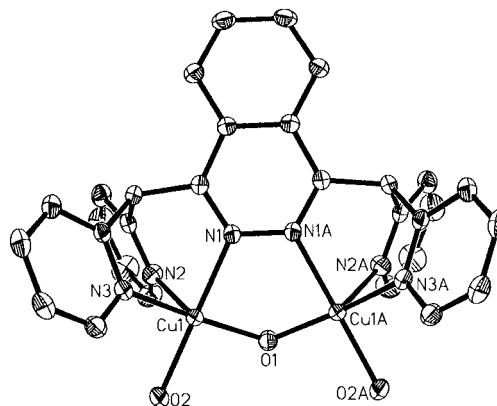


**Figure 4.** ORTEP diagram of the cation of **4**, showing 50% probability ellipsoids. Hydrogen atoms have been omitted for clarity.

from a tosylate anion in the crystal lattice makes a long interaction of  $2.789(4)$  Å with the sixth coordination site. The electronic spectrum of **4** has two bands in the visible region centered at 650 and 960 nm with an intensity ratio of approximately 2:1. These data are consistent with square-pyramidal coordination for the copper ions in solution as well as the solid state.<sup>31,32</sup>

The reaction of zinc tosylate with bdptz in the presence of 1 equiv of sodium hydroxide produced  $[\text{Zn}_2(\mu\text{-OH})(\mu\text{-H}_2\text{O})(\text{bdptz})(\text{H}_2\text{O})_2](\text{OTs})_3$  (**5**). The dizinc center in **5** is bridged by the phthalazine moiety of the bdptz ligand, a water molecule, and a hydroxide ion. The bridging water molecule is most uncommon in dizinc(II) complexes. Each zinc ion is further ligated by two pyridine donors from the bdptz ligand, and a water molecule occupies the remaining terminal coordination site on each metal. An ORTEP diagram of **5** is shown in Figure 5. Complex **5** is isostructural with a hydroxide-bridged dinickel complex of bdptz reported previously.<sup>19</sup>

The utility of the bdptz ligand for assembling dinuclear complexes of several biologically relevant transition metal ions

(31) Duggan, M.; Ray, N.; Hathaway, B.; Tomlinson, G.; Brint, P.; Pelin, K. *J. Chem. Soc., Dalton Trans.* **1980**, 1342–1348.

(32) Karlin, K. D.; Hayes, J. C.; Juen, S.; Hutchinson, J. P.; Zubieta, J. *Inorg. Chem.* **1982**, *21*, 4106–4108.

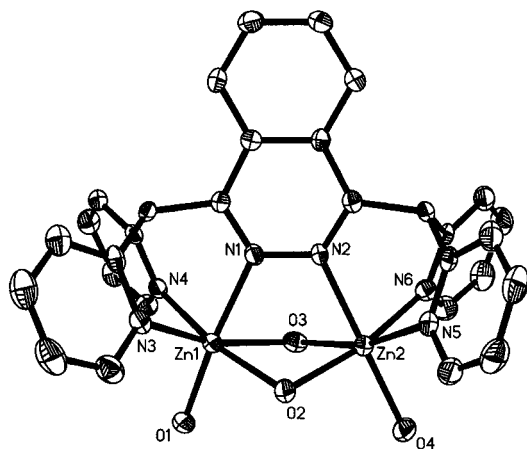


**Figure 5.** ORTEP diagram of the cation of **5**, showing 50% probability ellipsoids. The hydrogen atoms have been omitted for clarity.

is exemplified in the complexes presented here. Although the ligand favors the formation of pseudooctahedral complexes, other coordination geometries can be accessed. In addition to

the coordination flexibility of the complexes, a range of intermetallic distances and a variety of exogenous ligands can be supported by this system. The potential of the dinuclear bdptz complexes to serve as both structural and functional models for metalloenzymes has been realized in the case of the dinickel bdptz complexes.<sup>19,29,30</sup> Work is currently in progress in this laboratory to modify the bdptz ligand for further investigation of the properties of phthalazine-bridged metal centers as they relate to metalloenzyme active sites.

**Acknowledgment.** This work was supported by grants from the National Science Foundation and the National Institute of General Medical Sciences. We are grateful to Dr. Weiming Bu for assistance with the crystallographic analysis of **5**. A.M.B. thanks the NIH for a predoctoral fellowship.

**Supporting Information Available:** Fully labeled ORTEP diagrams of complexes **1–5** and X-ray crystallographic Tables S1–S25 in CIF format. This material is available free of charge via the Internet at <http://pubs.acs.org>.

IC000889K